

Comparative analysis of the results from static strength calculations and strength tests of an Y25Ls-K bogie frame

Svetoslav Slavchev^{1,*}, Vladislav Maznichki¹, Valeri Stoilov¹, and Sanel Purgic¹

¹Technical University – Sofia, “Railway engineering“ Department, 8 Kliment Ohridski Blvd., 1172 Sofia, Bulgaria

Abstract. The comparative analysis is based on the results of the static strength analysis of an Y25Ls-K bogie frame and the tests that have been carried out. Strength calculations have been made using the Finite Elements Method at the Department of Railway Engineering at the Technical University – Sofia and the tests of the bogie frame have been conducted in VUZ Testing laboratory in the Czech Republic. It was found out that the stress results are very similar, especially in the areas with maximal values. This proves that a suitable calculation model with a relatively small number of finite elements can be developed. This allows us to solve a wide range of problems concerning the improvement of the bogie frame with similar construction.

1 Introduction

This paper presents a comparative analysis of the static strength analysis and tests conducted on supporting steel structure of an Y25Ls-K bogie frame.

Strength calculations have been made using the Finite Elements Method [1, 2] at the Department of Railway Engineering of the Technical University – Sofia. The tests of the Y25Ls-K bogie frame have been carried out in the Výzkumný Ústav Železniční a.s.- VUZ Testing laboratory in the Czech Republic [3].

Theoretical and experimental studies have been done in full compliance with European standard EN 13749:2011 [4], EN 12663-2:2010 [5], TSI “Rolling stock” [6], and Leaflets 510-3 and 615-4 [7, 8] of the International Railway Union (UIC). According to those documents 13 load cases for study of stresses and displacements in the bogie frame construction are provided. Due to the limited size of the paper it presents only the results of five load cases marked in Table 1 with S1-S5. It should be noted that the number of points where the comparison is carried out is also limited. Only those that have relatively high stress values or are located in zones with section changes were studied.

2 Loading methodology

In accordance with the international requirements, each newly-built bogie is subjected to theoretical and native studies to demonstrate the strength of its structure. Types and conditions of loading are regulated by the European Standard EN 13749:2011 [4], the TSI [6] and the Leaflets of International Railways Union (UIC) 510-3 and 615-4 [7, 8]. According to the documents cited, the size and direction of the forces acting on the bogie depend on the load case (Fig. 1).

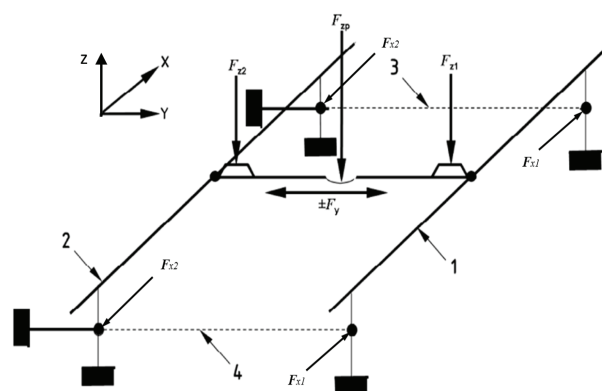


Fig. 1. Forces acting on bogie frame according to [4].

The forces acting on the bogie frame are defined in equations given in [4, 10], as follows:

• *Vertical forces*

$$F_z = 4Q_0 - m^+g. \quad (1)$$

In the case when the force is applied only to the pivot:

$$F_{zc} = 2F_z. \quad (2)$$

For cases when the force is applied to both the pivot and one sidebearer:

$$F_{zc1} = 1,5F_z(1 - \alpha); \quad (3)$$

$$F_{zc2} = 1,5F_z\alpha. \quad (4)$$

where: F_z – total vertical load supported by the bogie; Q_0 – static vertical force at the level of the wheel for a loaded wagon, for axle load $p_0=22,5$ t: $Q_0 = 0,5p_0g = 110$ kN; m^+ – bogie mass (4128 kg); g – acceleration due to gravity; F_{zc} – force applied only to the pivot;

* Corresponding author: slavchev_s_s@tu-sofia.bg

F_{z1} and F_{z2} – forces applied to the sidebearers. For UIC service with a distance between the sidebearers of 1,7 m, α is taken as 0,3. F_{bz} – vertical brake force defined in accordance to [10].

- *Transverse force*

$$F_y = 20 + (F_z + m^+g)/3. \quad (5)$$

- *Longitudinal lozenging forces*

$$F_x = 0,1(F_z + m^+g). \quad (6)$$

F_{bx} – longitudinal brake force defined in accordance with [10]. Brake force depends on the type of frame structure (axle box guidance, type of brake rigging etc. [10]).

- *Twist loading g^+* – the bogie frame should withstand the loads resulting from a track twist of 10 ‰.

Summing up the results of the equations given above, the following load cases combining the calculated forces (in kN) are obtained (Table 1).

Table 1. Applied load cases. All forces in [kN].

	F_{z2}	F_{z1}	F_{z1}	F_y	g^+	F_x	F_{bx}	F_{bz}
S1		801,9						
S2		421,0	180,4		+10 ‰			
S3		421,0	180,4		-10 ‰			
S4	180,4	421,0			+10 ‰			
S5	180,4	421,0			-10 ‰			
S6		421,0	180,4	167,2				
S7	180,4	421,0		-167,2				
S8		601,4				44,1		
S9		601,4				-44,1		
S10		400,9				202,6		
S11		400,9				-202,6		
S12		481,1					98,8	24,7
S13		481,1					-98,8	-24,7

3 Calculation models

From the analysis of the design documentation we have determined the bearing elements of the structure, the materials from which it is built and the technology of manufacturing (type of welds, additional machining, etc.). On the basis of this, the calculation models were designed [9] as shown in Fig. 2.

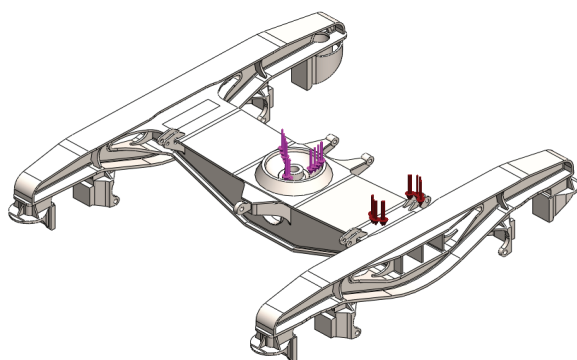


Fig. 2. Calculation model.

In this model the finite elements mesh is compressed (1 374 520 nodes and 843 616 elements), the maximum size of finite elements is 15 mm (Fig. 3), which shows a very good density of the analysed quantities.

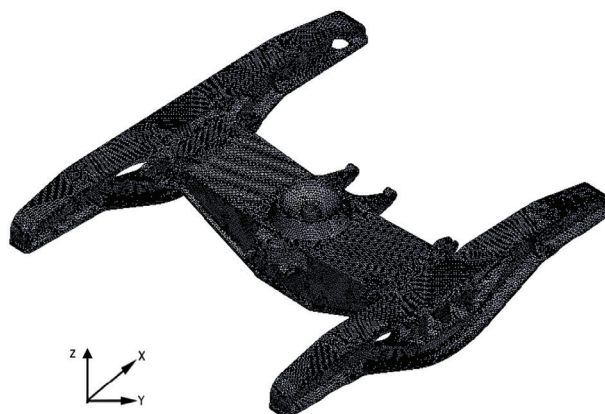


Fig. 3. Finite elements mesh of calculation model.

4 Results analysis

During the tests, stresses in terms of value and distribution, similar to those obtained theoretically, have been registered. A comparative analysis of the results is presented in Table 2 where the following indications are used: the strain gauge number/number of its corresponding element in the calculation model (Fig. 4), the test results in MPa are presented in the same row; σ_x , σ_y , and σ_z are the components of the stress tensor (7) on the main inertia axes x , y , z in MPa:

$$\sigma_{ij} = \begin{bmatrix} \sigma_x & \tau_{yx} & \tau_{zx} \\ \tau_{xy} & \sigma_y & \tau_{zy} \\ \tau_{xz} & \tau_{yz} & \sigma_z \end{bmatrix}; \quad (7)$$

von Mises stress results from FEM-calculation, von Mises stresses calculated with equation (8);

$$\sigma_{vM} = \sqrt{\frac{(\sigma_x - \sigma_y)^2 + (\sigma_y - \sigma_z)^2 + (\sigma_z - \sigma_x)^2 + 6(\tau_{xy}^2 + \tau_{yz}^2 + \tau_{zx}^2)}{2}} \quad (8)$$

S1- S5 are codes of analyzed load cases.

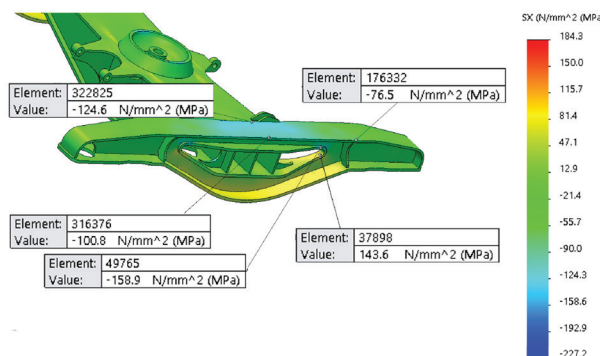


Fig. 4. Stress values obtained in elements corresponding to strain gauges

Table 2. Compared stress values.

DMS/Element	S1	S2	S3	S4	S5	max	min
T111/316376	-85	-47	-51	-70	-75	-47	-85
σ_x	-100,8	-61,4	-66,5	-87	-92,1	-61	-101
σ_y	-0,1	0,1	0,1	0	0,1	0	0
σ_z	0	0	0	-0,1	-0,1	0	0
von Mises	100,8	92,6	66,5	87	92,1	101	67
T112/322825	-119	-68	-65	-126	-119	-65	-126
σ_x	-124,6	-63,5	-57,5	-121,2	-115,2	-58	-125
σ_y	0	-0,8	-0,7	-1,4	-1,3	0	-1
σ_z	0	-0,1	-0,1	-0,1	-0,1	0	0
von Mises	124,6	113	57,1	120,4	114,5	125	57
T312/314726	-112	-123	-131	-64	-66	-64	-131
σ_x	-124,2	-121,2	-128,2	-59,6	-66,6	-60	-128
σ_y	0,1	-1,7	-1,7	-0,9	-0,9	0	-2
σ_z	0	-0,2	-0,2	-0,1	-0,1	0	0
von Mises	124,3	65,9	127,4	59,1	66,2	127	59
T213/176332	-76	-39	-24	-70	-58	-24	-76
σ_x	-76,5	-57,9	-36,9	-76,4	-55,4	-37	-77
σ_y	-0,8	-0,7	-0,3	-1	-0,6	0	-1
σ_z	0	-0,1	0	0	0,1	0	0
von Mises	76,1	73,7	36,7	76	55,1	76	37
T214/157611	-85	-76	-56	-91	-76	-56	-91
σ_x	-59,4	-42	-14,5	-74,6	-47	-15	-75
σ_y	-0,5	-0,7	-0,3	-1	-0,7	0	-1
σ_z	0	0,1	0	0,1	0	0	0
von Mises	59,1	65,4	14,4	74,1	46,7	74	14
T315/305644	-84	-77	-56	-37	-48	-37	-84
σ_x	-74,2	-61,9	-69,6	-45	-52,8	-45	-74
σ_y	-2,4	-2	-2,1	-1,7	-1,8	-2	-2
σ_z	0,2	0,5	1	0,1	0,6	1	0
von Mises	76,4	43,5	72,2	46,5	54,7	76	44
T316/309615	70	59	89	33	45	89	33
σ_x	73,1	65,4	81,4	30,4	46,4	81	30
σ_y	0	0	-0,1	0	-0,1	0	0
σ_z	17,5	16,1	22,1	6,8	12,8	22	7
von Mises	88,8	49,4	102	36,6	58,4	102	37
T119/246268	87	49	51	82	84	87	49
σ_x	119,4	64,4	64,3	108,7	108,7	119	64
σ_y	84,1	44,3	44,6	73,7	74,1	84	44
σ_z	-1	-1	-1	-1,5	-1,5	-1	-2
von Mises	107,2	97,1	58	97,6	97,6	107	58
T319/405348	92	87	88	52	52	92	52
σ_x	119,4	109,8	109,2	64,4	63,9	119	64
σ_y	83	72	70,7	42,2	41	83	41
σ_z	-0,1	0,1	0	0,1	0	0	0
von Mises	106,1	55,9	95,9	56,7	56,1	106	56
T322/238708	58	47	33	34	41	58	33
σ_x	27,9	47,6	42	0,7	-5	48	-5
σ_y	0,5	0,5	0,7	0,5	0,6	1	1
σ_z	1,1	2,2	1,8	-0,1	-0,4	2	0
von Mises	28,9	17,2	43,5	1,8	5,7	44	2
T32/467786	-117	-102	-163	-53	-83	-53	-163
σ_x	-130,5	-111,7	-147,2	-48,7	-84,2	-49	-147
σ_y	-0,6	-0,7	-1	-0,3	-0,6	0	-1
σ_z	0,2	0	-0,1	0	-0,1	0	0
von Mises	130,7	73	147,2	48,6	84,2	147	49
T325/263874	84	81	76	32	55	84	32
σ_x	65,7	54,9	59,4	36,4	40,9	66	36
σ_y	1,2	1,1	1,2	0,7	0,8	1	1
σ_z	12,9	11,4	12,8	7,3	8,8	13	7
von Mises	79	50,7	72,8	43,9	50,1	79	44
T229/198779	-89	-48	-57	-57	-69	-48	-89
σ_x	-23,2	-11,6	-14,4	-12,4	-15,2	-12	-23
σ_y	-53,9	-29	-31,5	-30,5	-33	-29	-54
σ_z	0,1	0	0	0,1	0	0	0
von Mises	75,5	46,3	44,8	42	47	76	42
T330/379240	82	52	41	43	47	82	41

σ_x	-1,5	-1,3	-1,5	-1,3	-1,5	-1	-2
σ_y	61,5	37,2	37,9	35,9	36,5	62	36
σ_z	0,7	0,3	0,4	0,3	0,4	1	0
von Mises	64,4	38,3	39,7	37,4	38,3	64	37
T430/377102	82	41	51	45	42	82	41
σ_x	-2	-1,7	-1,6	-1,7	-1,6	-2	-2
σ_y	58	37,5	36,6	36,5	35,6	58	36
σ_z	0,8	0,5	0,4	0,4	0,4	1	0
von Mises	61,1	38,7	38,4	38,4	37,3	61	37
T331/188444	108	21	218	18	123	218	18
σ_x	12,8	8,2	14,3	4,3	10,3	14	4
σ_y	129,7	91,5	141,3	47	96,8	141	47
σ_z	12,7	8	13,6	4,5	10,1	14	5
von Mises	137,7	104	150,4	49,7	104,1	150	50
T431/297427	128	206	2	112	5	206	2
σ_x	13,6	16,3	9,4	11,4	4,6	16	5
σ_y	132,6	146,1	95,9	97,9	47,7	146	48
σ_z	13,9	15,5	9,5	11	4,9	16	5
von Mises	141	49,1	100,3	105	50,1	141	49
T132/84072	-136	-67	-87	-118	-150	-67	-150
σ_x	-143,3	-77	-78,4	-131	-132,4	-77	-143
σ_y	3,9	-0,2	2,1	-1,4	1	4	-1
σ_z	-69,9	-39,1	-40,3	-65,8	-67	-39	-70
von Mises	195	179,7	106,8	175,5	179,9	195	107
T232/49765	-172	-111	-77	-174	-137	-77	-174
σ_x	-158,9	-81,2	-82,2	-136,3	-137,4	-81	-159
σ_y	5,6	3,5	-1,3	6,1	1,3	6	-1
σ_z	-70,8	-35,2	-33	-58,8	-56,7	-33	-71
von Mises	206,2	148,7	100,5	178,4	172,4	206	101
T237/37898	155	95	68	161	124	161	68
σ_x	143,6	77,8	80,4	136,6	139,2	144	78
σ_y	-12,3	-2,8	-5,3	-5,8	-8,4	-3	-12
σ_z	69,3	37,5	40,5	66,7	69,7	70	38
von Mises	204,6	162,9	114,7	191,1	197,6	205	115

The analysis of the data in Table 2 shows that there is a very good match of the results. Differences in stress values can be explained by the simplifications adopted in the modeling: the way of gluing and positioning of the strain gauges; measuring errors of equipment; inaccuracies in the manufacturing of the bearing structure; technological deviations of the material; the presence of serious stress notches etc.

Table 3 presents data for the forces applied in five load cases considered in the paper (Figures 5 and 6). In vertical direction, very good matching can be observed and the test forces differ slightly from the calculated ones. This can be explained by the errors of the measuring equipment and the asymmetry of the structure.

Table 3. Applied vertical forces in kN.

	S1	S2	S3	S4	S5
F_{z1}	-399,0	-223,5	-223,9	-377,0	-376,8
F_{z2}	-399,9	-376,3	-376,8	-222,4	-224,1
sum F_z	-799,0	-599,8	-600,7	-599,4	-600,9
F_z FEM	801,9	601,4	601,4	601,4	601,4

Table 4 shows the reaction data R_{z1} - R_{z4} in bearings in the vertical direction (Figures 5 and 6) for the asymmetrical load cases S2 to S5. A very good match can be seen, excluding the values of the bearing reaction, where the track twist is imitated.

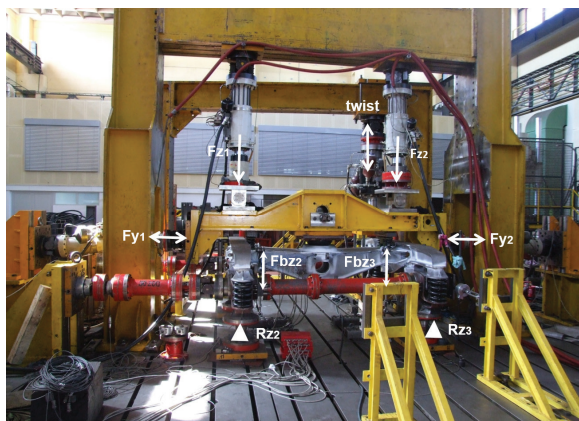


Fig. 5. Test rig at Výzkumný Ústav Železniční a.s. (VUZ) [3].

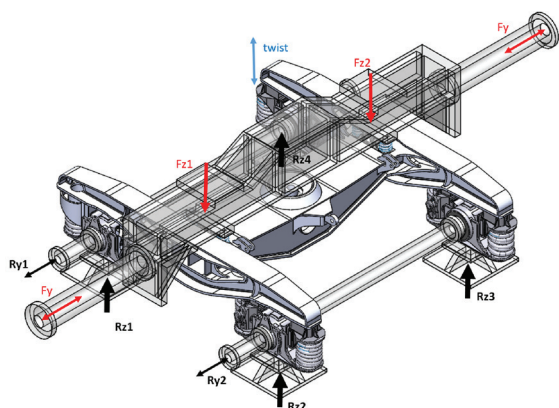


Fig. 6. Bearing reactions.

Table 4. Bearing reactions in [kN].

	R_{z1}	R_{z2}	R_{z3}	R_{z4}
S2	88,2	134,6	146,1	212,8
	101,5	123,2	172,0	224,3
S3	133,9	88,5	212,8	146,8
	123,2	101,8	204,7	151,7
S4	179,8	200,9	83,5	136,8
	177,4	199,2	96,2	148,6
S5	212,8	151,7	133,8	88,3
	199,0	177,8	128,9	76,0

This can be explained by a difference in the position where the frame displacement (as a consequence of the track twist) is applied. If the force is applied under the support of the measuring equipment, then the magnitude of the reaction would increase. Similarly, if the force is applied above the support, the magnitude of the reaction would decrease with the value of the force produced by the track twisting (Fig. 7).

5 Conclusions and recommendations

when summarizing the overall work done on this study the following conclusions and recommendations can be made:

1. Sophisticated calculation models for the strength analysis of the Y25Ls-K bogie frame have been

developed, consisting of 843 616 finite elements that accurately describe the geometry of the object.

2. In the process of strength testing minor design changes of the Y25Ls-K bogie frame were made.

3. The analysis of the results in Tables 2 and 3 shows that the stress distribution obtained theoretically is very close to the stress distribution recorded in the test.

4. The relative error of stress results is relatively small, which allows for developed calculation models to be used in order to study other similar bogie frame designs as well as to optimize the tested bogie.

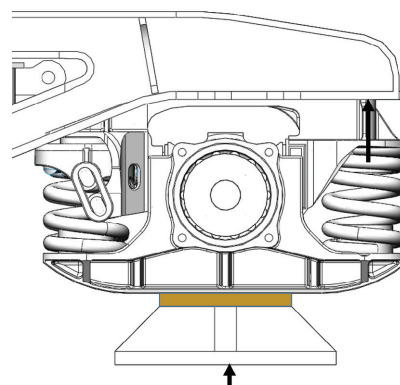


Fig. 7. Reaction under the support.

References

1. O. Zenkiewicz, *The Finite Element Method in Engineering Science*, McGraw-Hill, London, (2002)
2. L. Segerlind, *Applied Finite Element Analysis*, 2nd edition, Wiley, New York, (1984)
3. VUZ Plc., Test report Strength tests of bogies and their components: Non-destructive testing – Magnetic particle test (MT) - Bogie frame Y25Ls-K, VUZ Plc., Czech Republic, (2017)
4. EN 13749:2011 Railway applications. Wheelsets and bogies. Method of specifying the structural requirements of bogie frames, (2011)
5. EN 12663-2:2010 Railway applications. Structural requirements of railway vehicle bodies. Freight wagons, (2010)
6. Technical specifications for Interoperability (TSI) - Rolling stock: Freight wagons. European Union, Agency for Railways, (2013)
7. UIC Leaflet 615-4, Motive Power Units - Bogies And Running Gear - Bogie Frame Structure Strength Tests, 2nd edition, UIC, (2003)
8. UIC Leaflet UIC 510-3, Wagons - Strength Testing Of 2 And 3-axle Bogies On Test Rig, UIC, (1989)
9. R. Tenchev, *User guide for COSMOS/M*, Technical University - Sofia, (2010)
10. K. Velkov, O. Krastev, *Technologies and systems for train control*, Technical University - Sofia, (2010)